

Review article

Nanoparticles for drug delivery: The need for precision in reporting particle size parameters

Marie Gaumet, Angelica Vargas, Robert Gurny, Florence Delie *

Department of Pharmaceutics and Biopharmaceutics, University of Geneva, University of Lausanne, Geneva, Switzerland

Received 27 April 2007; accepted in revised form 1 August 2007

Available online 7 August 2007

Abstract

Polymeric drug-loaded nanoparticles have been extensively studied in the field of drug delivery. Biodistribution depends on the physicochemical properties of particles, especially size. The global message from the literature is that small particles have an enhanced ability to reach their target. The present review highlights the difficulties in validating the data from biodistribution studies without accurate particle size determination.

© 2007 Elsevier B.V. All rights reserved.

Keywords: Nanoparticle; Biodistribution; Size determination; Drug carrier

1. Introduction

The development of a drug delivery system faces several challenges: reaching the target site, which is often far away from the administration site (drug targeting), remaining at the target site to deliver the drug, preferably in a time controlled manner, limiting the drug's adverse effects and ensuring biocompatibility. Polymeric particles used for drug delivery are defined as colloidal systems made of solid polymers [1]. The need for intravenous (IV) formulations and the advantage of enlarging surface contact with an external medium to control release kinetics have encouraged the development of nanoparticles (<1 µm). Before reaching the target site, nanoparticles undergo a biodistribution step possibly after crossing epithelial barriers and travelling through the vascular bed. After administration, small particles (<20–30 nm) are eliminated by renal excretion [2,3]. Larger particles can be rapidly taken up by the mononuclear phagocytic system (MPS) cells present in

the liver, the spleen, and to a lesser extent, in the bone marrow. Nanoparticles of 150–300 nm are found mainly in the liver and the spleen [4], whereas particles of 30–150 nm are located in bone marrow [5], the heart, the kidney and the stomach [6]. Nanoparticles can escape from the circulation through openings, also called fenestrations, of the endothelial barrier (Fig. 1). Table 1 summarizes the data regarding fenestration size for the main organs.

Although nanoparticles should be smaller than 150 nm to cross the endothelial barrier, the literature often reports the penetration of particles larger than the limits of fenestrations. Indeed, fenestrations and the vasculature can undergo modifications under various pathological conditions [7]. For instance, tumor growth induces the development of neovasculature characterized by discontinuous endothelium with large fenestrations of 200–780 nm [8] allowing nanoparticles passage. Depending on the reports, the “ideal” size requirements for nanoparticles developed for cancer treatment are between 70 and 200 nm [9].

Do we need to design smaller and smaller carriers? Which particle size best suits each individual target? Is particle size correctly assessed? These are some of the questions that scientists face trying to design the “ideal” colloidal drug carrier. Nowadays, the race for ever smaller

* Corresponding author. Department of Pharmaceutics and Biopharmaceutics, School of Pharmaceutical Sciences, University of Geneva, University of Lausanne, 30, Quai E. Ansermet, CH-1211 Geneva 4, Switzerland. Tel.: +41 22 379 65 73; fax: +41 22 379 65 67.

E-mail address: Florence.delie@pharm.unige.ch (F. Delie).

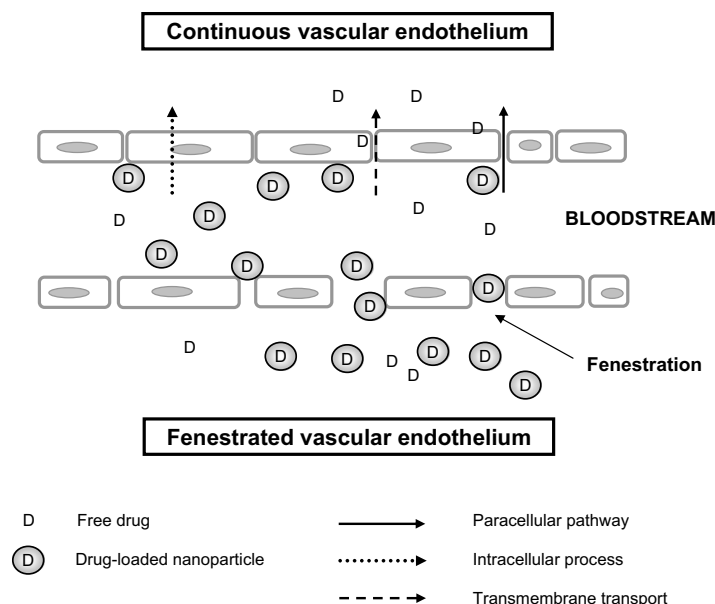


Fig. 1. Vascular escape of nanoparticles in either continuous or fenestrated tissues. Healthy tissues are characterized by continuous vascular endothelium preventing nanoparticles extravasation. The drug (D) released from the nanoparticles can reach the extravascular compartment by different pathways represented by the arrows. On the contrary, in pathological situations, such as cancer or inflammatory tissues, the vascular endothelium is fenestrated. Nanoparticles can go through fenestrations thus enhancing drug penetration in tissues.

Table 1
Claimed sizes of fenestrations of the vasculature in different organs and some pathologies

Organ or pathological situation	Fenestration size	Animal model	Ref.
Kidney	20–30 nm	Guinea-pig, rabbit, rat	[2,3,34]
Liver	150 nm	Mice	[35]
Spleen	150 nm	Mice	[35,36]
Lung	1–400 nm	Dog	[80]
Bone marrow	85–150 nm	Guinea-pig, rabbit, rat	[2,5]
Skeletal, cardiac and smooth muscle	≤6 nm	Mice	[37]
Skin, subcutaneous and mucuous membrane	≤6 nm	Mice	[37]
Blood–brain barrier	No fenestrations	–	[38,39]
Tumor ^a	200–780 nm	Mice	[8,40]
Brain tumor ^b	100–380 nm	Rat	[41]
Inflamed organs	80 nm–1.4 μm	Hamster	[81]

These values result from indirect measurements and should therefore be used with caution.

^a Implanted tumor.

^b Intravenously inoculated tumor.

carriers has begun. From a technological standpoint, polymeric particles can hardly be made smaller than 5 nm [10]. To underline the major role of nanoparticle size, the difficulties of obtaining accurate measurements of size will be first highlighted. A search of the literature, it becomes obvious that thorough size determination is frequently missing, leading to the misinterpretation of data and generating conflicting results from similar studies. This aspect is dis-

cussed through several case studies in the second part of this article.

2. Size determination: not straightforward

Size influences both the clearance and the biodistribution of nanoparticles, but this parameter is not always perfectly controlled and often poorly described in most publications. Many tools based on different physical principles are currently available to measure particle sizes smaller than 1 μm (Table 2). Thus, data from the literature are difficult to compare when different methods have been used.

Light scattering (LS), also called photon correlation spectroscopy (PCS), is a rapid method for determining the mean size, the size distribution and the polydispersity index (PI) of a sample. This method is well adapted for routine measurements. From the interaction with light, nanoparticle size is determined, generally at an observation angle of 90°. The calculation model is based on the equivalent sphere principle, in which each particle is viewed as a sphere. Thus, the presence of a few aggregates will tremendously increase the mean size. The results should be interpreted cautiously because several parameters such as viscosity or pH of the suspension medium, temperature, concentration and particle sedimentation may influence the data. Moreover, the method may not be reliable in analysing samples with a mixed population of size. To improve the accuracy in size determination, working with variable angle systems is recommended [11]. LS is designed for colloidal particles, and is therefore not suitable for particles larger than 1 μm, except when a monomodal popula-

Table 2
Main characteristics of particle size measurement methods

Method ^a	Principle	Measured size ^b	Limitations
LS	Light interaction	50 nm–1 μ m	Non-appropriated for very polydisperse populations Indirect method Great influence of aggregates or larger particles Many influencing parameters
LLD	Light interaction	1–1000 μ m	High amount of sample required Indirect method
SEM, TEM	Microscopy	50 nm–100 μ m	Time consuming Influence of the preparation sample
AFM	Microscopy	10 nm–1 μ m	Sampling Non-automated Complexity of the set up Image treatment Subjective
ANUC	Centrifugation	–	Complex data processing
FFF	Elution	20 nm–1 μ m	Difficult to handle Optimization needed for each kind of particles
CE	Electrophoresis	20–500 nm	Complexity of the set up
PCH, SEC	Chromatography	<100 nm	Long steps of optimization Time consuming

^a LS, light scattering; LLD, laser light diffraction; SEM, scanning electron microscopy; TEM, transmission electron microscopy; AFM, atomic force microscopy; ANUC, analytical ultracentrifugation; FFF, field flow fractionation; CE, capillary electrophoresis; PCH, packed column hydrodynamic; SEC, size exclusion chromatography.

^b Size range for which the method can be applied with accuracy.

tion with a narrow size distribution and slow sedimentation rate is analysed. Particles larger than 1 μ m may be characterized by laser light diffraction (LLD), which presents two main limitations: the large amount of sample required and the over-estimation of small size population (smaller than 500 nm). Scanning electron microscopy (SEM) allows the observation of the sample after drying and coating with a thin layer of gold or platinum [12]. This method allows for a resolution between 3 and 5 nm, and even to 1 nm with some advanced microscopes. Other techniques remain barely exploited owing to the difficulty of experimentation with the instrumentation, and their high cost. Included among these techniques are transmission electron microscopy (TEM), which requires several steps of sample preparation [13], atomic force microscopy (AFM), which is more appropriate for surface analysis [14], the analytical ultracentrifugation (ANUC) which results in complex data analysis [15], field flow fractionation (FFF), a more recent technique but not appropriate for all types of nanoparticles [16] and capillary electrophoresis (CE) [17]. Chromatographic procedures may also be performed to evaluate nanoparticle size but they are time consuming, difficult to optimize, and more appropriate for sizes under 100 nm [18].

From this list, the most cited techniques in the literature are the SEM and LS (Table 3). SEM provides the most direct picture of nanoparticles, giving information about the size, shape and other general aspects. Particles with a size under 100 nm may be difficult to observe, depending

on the microscope and the set up. During the drying step, particles may shrink, leading to an under-estimation of their actual diameter. Particle sizing with SEM requires image treatment of a large number of particles, thus making this method subjective, tedious and time consuming.

Data processing of LS measurements also presents some difficulties. Size measurement is based on the calculation of mean size from a large number of particles. The size, calculated from a single data set, is usually presented along with standard deviation (SD). Standard deviation is a statistical calculation that indicates the distribution of the size around the mean. Typically, size measurements are repeated several times on the same sample. Most of the results given by the data processors of LS equipment give the SD on the means obtained at each run. Therefore, the data do not represent the variation on the whole particle population but the variation of the median on the same sample. This may be quite misleading and a typical result such as 126 ± 2 nm found in the literature does not mean that all the particles are between 124 and 128 nm but that 2 nm represents the error made on three measurements and not the distribution of the particle population. A schematic representation of size distribution data is given in Fig. 2. Size distribution can be monomodal (one population) or plurimodal (several populations), and monodisperse (narrow distribution) or polydisperse (broad distribution). For instance, a batch with a mean size of 300 nm and described in the literature as “monodisperse” does not mean that all of the particles measure 300 nm but that

Table 3
Critical analysis of *in vitro* studies classified according to polymer types

Polymer	Mean size \pm SD (PI [*]) (nm)	Reference quote	Critical comment	Ref.
Cs	155–289 ^m 100 \pm 10 ^s 290 \pm 7 ^s	“highly monodispersed nanoparticles” “no difference in the particles size”	TEM data not shown TEM images show sizes from 60 nm to 200 nm pH unknown for measurements	[42] [26] [43]
CS–DNA	\sim 200 ^s		No accurate value given, pH unknown	[44]
PCA–PEG	149.9 \pm 7.5 ^s		No information regarding the size distribution	[45]
PCL	200–300 ^m	“narrow size distribution”	SEM showing particles from 100 to 800 nm	[46]
PCL–PEG	247 \pm 83 ^s	“no significant difference in size”	No SEM, no information about size distribution	[47]
PGA–CS	365.5 \pm 5.1 ^s \sim 50 ^s		No information regarding the size distribution TEM data not shown, no accurate value given	[48] [49]
PLA	600–7900 ^m 387 \pm 44 ^s	“the size distribution [...] quite uniform” “small standard deviation which indicates narrow size dispersity”	No SEM SEM data not shown	[50] [51]
PLA–mePEG	331 \pm 11 ^s		Only one characterization technique	[52]
PLA–pDMAEMA	651 \pm 4 ^s (0.2)		High PI	[53]
PLA–PEG	226 \pm 60 ^s (0.105) 196 \pm 20 ^s 210 \pm 71 ^s	“no difference in the particles size” “no significant difference in size”	pH unknown for measurements No SEM, no information about size distribution	[43] [47]
PLA–PEI	307 \pm 27 ^s (0.19)		High PI	[55]
PLGA	321 ^s (0.132) 310 ^s (0.14) 562 \pm 18 ^s 210 \pm 12 ^s (0.59 \pm 0.11) 315.1 \pm 26.1 ^s 148.7–298.2 ^m (0.115–0.224) 600–7900 ^m	“uniformity of the particle size distribution” “the size distribution [...] quite uniform”	No SEM SEM: size distribution appears bimodal No information regarding the size distribution High PI Only one characterization technique TEM: high polydispersity	[27] [56] [57] [58] [59] [60]
PLGA–PEG	252 \pm 85 ^s	“no significant difference in size”	No SEM, no information about size distribution	[47]
PMAA–PEG	475 ^s		Method for size determination not mentioned	[61]
PS	77.4 \pm 32.8 ^s		Only one characterization technique, high standard deviation	[22]
PVAm, PNVA, PNIPAAm, PMAA	500–750 ^s		Only one characterization technique	[62]
SLN	146–254 ^m (0.12–0.21)		Only one characterization technique	[63]
No specification	168–489 ^m		Only one characterization technique	[64]

CS, chitosan; DNA, deoxyribonucleic acid; mePEG, methoxypoly(ethylene glycol); PCA, poly(cyanoacrylate); PCL, poly(caprolactone); pDMAEMA, poly(dimethylamino)ethyl methacrylate; PEG, poly(ethylene glycol); PEI, poly(ethylenimine); PGA, poly- γ -glutamic acid; PLA, poly(lactic acid); PLGA, poly(lactide-co-glycolide) acid; PMAA, poly(methacrylic acid); PNIPAAm, poly(*N*-isopropylacrylamide); PNVA, poly(*N*-vinylacetamide); PVAm, poly(vinylamine); PS, polystyrene; SEM, scanning electron microscopy; SLN, solid lipid nanoparticles; TEM, transmission electron microscopy.

* Polydispersity index.

^m Multiple batches; size between the two given values.

^s Single batch.

the distribution is symmetric and centred around 300 nm. The latex particles used as a reference can be considered monodisperse, with a narrow size distribution. Usually, authors comment on size distribution using the polydispersity index (PI). The calculation of PI takes into account the

particle mean size, the refractive index of the solvent, the measurement angle and the variance of the distribution [19]. What is a “good” polydispersity index? If a scale from 0 to 1 is considered, a PI lower than 0.1 might be associated with a high homogeneity in the particle population,

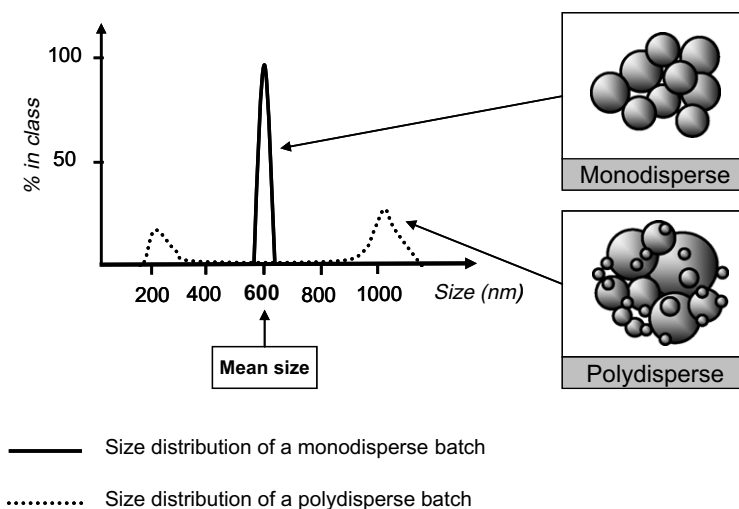


Fig. 2. Schematic representations of two nanoparticle batches corresponding to a monodisperse population and to a bimodal polydisperse population. The graph represents the curves obtained for each batch after analysis by light scattering.

whereas high PI values suggest a broad size distribution or even several populations. Indeed, a linear correlation between the PI value and the true monodispersity of a sample cannot be drawn. Fig. 3 shows measurements made on PLGA (3a) and latex (3b) nanoparticles to compare the PI obtained by LS (detection angle of 90°) and the size distribution observed by SEM. Fig. 1, using an electron microscope (JSM-6300[®], JEOL, Japan), shows the PLGA nanoparticles. The sizes ranged from 100 nm to 1 μ m, clearly indicating a polydisperse distribution. The same batch measured by LS (Zetasizer[®] 3000, Malvern, UK) gave a mean size of 318 nm with PI of 0.093 (scale from 0 to 1), which suggests a monomodal distribution. Fig. 3b represents an SEM picture (microscope Philips[®] XL-30, Lancashire, UK) of a monodisperse batch of latex particles (Duke Scientific Corp., Palo Alto, CA). Whereas the picture shows a highly homogeneous batch, measurement on LS gave a PI of 0.12 suggesting a moderately homogeneous batch. This example underlines the difficulty

in assessing real size distribution in a batch and the necessity of combining several techniques.

The nature of the dispersive medium may also have a critical impact on size determination. In a recent study, chitosan nanoparticles were prepared and characterized by LS and TEM [20]. The size obtained by LS was 182 nm and $PI = 0.17$, whereas TEM observations suggested a size between 20 and 80 nm. Such differences cannot only be explained by the dry state of the nanoparticles during TEM analysis. Chitosan is a cationic polysaccharide with specific physicochemical properties varying according to pH. At neutral pH, chitosan chains are more condensed than at acidic pH. Therefore, as measurements were made in unbuffered water, it is expected that chitosan chains were elongated due to the acidic pH, thus giving a larger hydrodynamic diameter compared to measurements made in neutral environment or in dry state. Our experience with chitosan nanoparticles has shown that measurements at pH 4 by LS may be twice those assessed at pH 7.

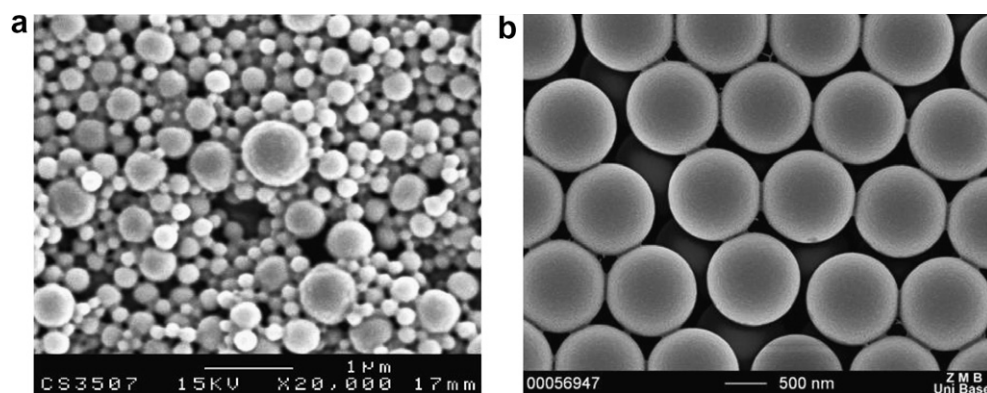


Fig. 3. SEM micrographs of two batches of particles. (a) Polydisperse PLGA nanoparticle batch. (b) Monodisperse latex particles. In parallel the same samples have been analysed by light scattering giving the following data: 318 nm ($PI = 0.09$) for the PLGA nanoparticle batch (a) and 1063 nm ($PI = 0.12$) for the latex particles (b).

To conclude, many methods are available to determine particle size, each of them based on a different physical theory and data processing method. Each technique has its own advantages and limitations; therefore, it is strongly recommended that at least two methods be combined to accurately characterize a batch [21]. To avoid interfering with the method, the measurement of hydrodynamic diameter is usually made in water or buffer. This is, however, not representative of the biological medium that the particles will meet after administration. Therefore, the size measured *in vitro*

may be far off from the actual size when in contact with proteins. An increase of up to 50% in the particle size upon contact with a protein-containing medium is generally observed due to aggregation phenomena or opsonization [22].

3. Critical analysis

The evidence that size influences particle biodistribution is based on size determination reported by different authors. However, in view of the difficulties encountered

Table 4
Critical analysis of *in vivo* studies classified according to polymer types

Polymer	Mean size \pm SD (PI*) (nm)	Reference quote	Critical comment	Ref.
CS	30 ^s	“highly monodispersed nanoparticles” “no difference in the particles size”	Extrapolation at infinite dilution, pH unknown	[6]
	100 \pm 10 ^s		TEM shows sizes from 60 to 200 nm	[26]
	290 \pm 7 ^s		pH unknown for measurements	[43]
HSA	340 \pm 8.6 ^s		Only one characterization technique	[28]
mePEG–PHDCA	80–243 ^m		Only one characterization technique	[65]
mPEG–PLA/ PLMA	21.7 ^s		Only one characterization technique	[66]
PBCA	270 \pm 30 ^s		Only one characterization technique	[67]
PCA–PEG	101.4 \pm 7.2 ^s		Difficulty to correlate TEM pictures and mean size	[68]
PEG–PPS	20–100 ^m		Only one characterization technique	[69]
PEI–DS	364 \pm 10 ^m (0.17)	“narrow size distribution”	SEM and TEM images are not clear	[70]
PLA	121–343 ^m (0.21–0.42)		Only one characterization technique, high PI	[24]
PLA–PEG	196 \pm 20 ^s	“no difference in the particles size”	pH unknown for measurements	[43]
PLA–PS–PEG	18–37 ^m		ANUC and LS but no visualization by SEM	[29]
pMAEA	292 \pm 22 ^s (0.3)	“monodispersed size distribution”	SEM data not shown, high PI	[71]
PLGA	660 \pm 20 ^s		Polydisperse	[72]
	134–159 ^m (0.050–0.099)		Only one characterization technique	[73]
	520–670 ^m		No information regarding size distribution	[65]
	300 \pm 5 ^s		Number of measured particles from SEM images not indicated	[74]
	170 \pm 12		PI not given	[75]
	–	“low polydispersity indices”	No size measurement	[76]
PLGA–mPEG	113.5 \pm 14.3 ^s (0.385)		High PI	[77]
PLGA–PEG	58–112 ^m (0.3–0.5)		High polydispersity, no SEM	[23]
	58–115 ^m		High polydispersity, no SEM	[30]
PL–PEG	100.5–372.7 ^m		Only one characterization technique	[78]
PS	77.4 \pm 32.8 ^s		Only one characterization technique, high standard deviation	[79]
PS–poloxamer	48–145 ^m		Only one characterization technique	[32]

ANUC, analytical ultracentrifugation; CS, chitosan; DS, dextran sulphate; HSA, human serum albumin; mePEG, methoxypoly(ethylene glycol); mPEG, monomethoxypoly(ethylene glycol); PBCA, poly(butylcyanoacrylate); PCA, poly(cyanoacrylate); PEG, poly(ethylene glycol); PEI, poly(ethylenimine); PHDCA, poly(cyanoacrylate-co-hexadecylcyanoacrylate); PLA, poly(lactic acid); PLGA, poly(lactide-co-glycolide) acid; PLMA, poly(lactic acid-co-mandelic acid); pMAEA, poly(methacrylic acid-co-ethylacrylate) copolymer; PPS, poly(propylene sulphide); PS, polystyrene; SEM, scanning electron microscopy; TEM, transmission electron microscopy.

^m Multiple batches; size between the two given values.

^s Single batch.

* Polydispersity index.

with these types of studies, some of the results appear questionable. Furthermore, few studies have evidenced the actual presence of particles in either blood or organs. Indeed, most of the biodistribution data were determined by indirect evaluations such as drug quantification or pharmacological effects. A non-exhaustive list of *in vitro* and *in vivo* studies over the past five years is presented in Table 3 and 4, respectively, where the size determination of the particles is the subject of specific remarks.

The main issue is the determination of size distribution. As mentioned earlier, mean size does not mean anything without proper determination of size distribution. For instance, Beletsi et al. studied the biodistribution of 10 batches of PLGA–PEG stealth particles with a the size range of 58–112 nm, after IV injection in mice [23]. In this study, the polydispersity varied from 0.3 to 0.5, implying wide distribution in all batches, and several populations of overlapping particles. Thus, the relationship between effect and size could not be ascertained. Similarly, Pegaz et al. recently studied the effect of size on the extravasation and the photothrombic activity of four batches of PLA nanoparticles loaded with meso(*p*-tetracarboxyphenyl)porphyrin [24]. The mean sizes were very close with very high PIs: 121 nm (PI = 0.42), 194 nm (PI = 0.21), 250 nm (PI = 0.30) and 343 nm (PI = 0.23). High PIs indicate that the actual sizes of the different batches were truly close and that overlapping may be expected. However, the authors concluded on the basis of their data that smaller particles were preferred. The differences in the efficiency of the different batches may as well be due to the presence of residual surfactant affecting surface properties and thus interaction with target cells. Indeed, different concentrations of poly(vinyl) alcohol were used as a stabilising agent to obtain different batches. Other studies claimed a very high homogeneity in size without giving either PI or size distribution, but only the standard deviation calculated from three measurements [25–28].

Investigations attempting to study the biodistribution of ultrafine nanoparticles have encountered several problems in accurate determinations of particle size. In a study with radiolabeled chitosan nanoparticles [6], size measurement was made impossible at the concentration used for *in vivo* experiments due to cluster formation in relation to chitosan adhesiveness. Therefore, the suspension was progressively diluted to reduce particle interactions. At infinite dilutions, a size of 30 nm was determined. First of all, one may wonder if this size represents the actual size of the particle once administered in the body as a more concentrated suspension. Furthermore, TEM data showed a polydisperse population. Finally, the pH at which the size was measured (LS) was not specified, in spite of its importance in chitosan particles. All these elements lead to the conclusion that the size of 30 nm, even though correct, may not be representative of the actual size in the *in vivo* situation. Indeed, such small particles should exhibit a relatively long circulation time. The biodistribution data, however, show that only 13% of the dose remained in blood after 30 min and 7% after 4 h.

Sun et al. compared the percentages of particles of different sizes made of either acrylate or polystyrene in the blood compartment 4 h after injection in mice [29]. The authors reported a size-biodistribution correlation for small nanoparticles measuring 18, 24 and 37 nm. Is it possible to observe differences in biodistribution between three batches having such small size differences and prepared from different compounds? Other biodistribution studies showed that particles of the same size reached different blood levels (2 h after IV injection) depending on the polymer, 60% for particles of PLGA–PEG measuring 58 nm [30] and less than 20% for particles of VP–NIPAAm measuring 45 nm [25]. In these two examples, parameters other than size, such as the nature of the polymer, appear to have contributed to their long-circulating properties. The literature provides several examples stressing the importance of parameters such as charge and hydrophilicity on particle–cell interactions [26,29–33]. Therefore, it is not proper to discuss size effects independently of other factors.

From the data gathered in Tables 3 and 4, two major inadequacies emerge: in 60% of the publications, only one characterization technique was used and in 70% no microscopic observations were presented. Furthermore, in 28% of the reports, particle populations were described as monodisperse, notwithstanding their broad size distribution. Finally, more than 10% of the reports did not present any information about size distribution. In the majority of published studies, particles are incorrectly or poorly characterized; therefore the correlation with biodistribution may be erroneous.

4. Conclusion

The literature provides evidence that size does matter when particle biodistribution is concerned. However, the size limits to target a specific organ and the involvement of other parameters in particle distribution still remain poorly understood, and may be in part due to inadequate particle characterization. Several methods are available to characterize particles, especially in terms of size, but none of them are fully satisfactory. Therefore, a combination of at least two methods, one of which should be a microscopic method, is highly recommended. Each indirect technique performed has obviously to be validated by using standard particles. Furthermore, polydispersity should be discussed carefully because overlapping might be expected. As a result, incorrect size measurement, and differences in particle surface, animal models and doses make comparison of data gathered from the literature difficult.

References

- [1] E. Allemann, R. Gurny, E. Doelker, Drug-loaded nanoparticles – preparation methods and drug targeting issues, *Eur. J. Pharm. Biopharm.* 39 (1993) 173–191.
- [2] R. Nakaoka, Y. Tabata, T. Yamaoka, Y. Ikada, Prolongation of the serum half-life period of superoxide dismutase by poly(ethylene glycol) modification, *J. Control. Release* 46 (1997) 253–261.

- [3] S.M. Moghimi, A.C. Hunter, J.C. Murray, Long-circulating and target-specific nanoparticles: theory to practice, *Pharmacol. Rev.* 53 (2001) 283–318.
- [4] S.M. Moghimi, Mechanisms of splenic clearance of blood cells and particles: towards development of new splenotropic agents, *Adv. Drug Deliv. Rev.* 17 (1995) 103–115.
- [5] S.M. Moghimi, Exploiting bone marrow microvascular structure for drug delivery and future therapies, *Adv. Drug Deliv. Rev.* 17 (1995) 61–73.
- [6] T. Banerjee, S. Mitra, S.A. Kumar, S.R. Kumar, A. Maitra, Preparation, characterization and biodistribution of ultrafine chitosan nanoparticles, *Int. J. Pharm.* 243 (2002) 93–105.
- [7] A. Hirano, T. Kawanami, J.F. Llana, Electron microscopy of the blood–brain barrier in disease, *Microsc. Res. Tech.* 27 (1994) 543–556.
- [8] S.K. Hobbs, W.L. Monsky, F. Yuan, W.G. Roberts, L. Griffith, V.P. Torchilin, R.K. Jain, Regulation of transport pathways in tumor vessels: role of tumor type and microenvironment, *Proc. Natl. Acad. Sci. USA* 95 (1998) 4607–4612.
- [9] G. Storm, S.O. Belliot, T. Daemen, D.D. Lasic, Surface modification of nanoparticles to oppose uptake by the mononuclear phagocyte system, *Adv. Drug Deliv. Rev.* 17 (1995) 31–48.
- [10] H. Kawaguchi, Functional polymer microspheres, *Prog. Polym. Sci.* 25 (2000) 1171–1210.
- [11] M. Borkovec, Measuring particle size by light scattering, in: K. Holmberg (Ed.), *Handbook of Applied Surface and Colloid Chemistry*, 2002, pp. 357–370.
- [12] W.E. Vanderlinde, Microscopy at the nanoscale, in: *Proceedings of the 30th International Symposium for Testing and Failure Analysis*, Worcester, Boston, Massachusetts, 2004.
- [13] C. Duclairoir, E. Nakache, Polymer nanoparticle characterization in aqueous suspensions, *Int. J. Polym. Anal. Charact.* 7 (2002) 284–313.
- [14] M.N. Ravi Kumar, U. Bakowsky, C.M. Lehr, Preparation and characterization of cationic PLGA nanospheres as DNA carriers, *Biomaterials* 25 (2004) 1771–1777.
- [15] H. Cölfen, Analytical ultracentrifugation of nanoparticles, *Coll. Chem.* 29 (2004) 101–116.
- [16] W. Fraunhofer, G. Winter, C. Coester, Asymmetrical flow field-flow fractionation and multiangle light scattering for analysis of gelatin nanoparticle drug carrier systems, *Anal. Chem.* 76 (2004) 1909–1920.
- [17] F.K. Liu, Y.Y. Lin, C.H. Wu, Highly efficient approach for characterizing nanometer-sized gold particles by capillary electrophoresis, *Anal. Chim. Acta* 528 (2005) 249–254.
- [18] C.H. Fischer, Chromatography of colloidal inorganic nanoparticles, *Surfact. Sci. Ser.* 80 (1999) 173–226.
- [19] D.E. Koppel, Analysis of macromolecular polydispersity in intensity correlation spectroscopy: the method of cumulants, *J. Chem. Phys.* 57 (1972) 4814–4820.
- [20] Y. Wu, W. Yang, C. Wang, J. Hu, S. Fu, Chitosan nanoparticles as a novel delivery system for ammonium glycyrrhizinate, *Int. J. Pharm.* 295 (2005) 235–245.
- [21] A. Bootz, V. Vogel, D. Schubert, J. Kreuter, Comparison of scanning electron microscopy, dynamic light scattering and analytical ultracentrifugation for the sizing of poly(butyl cyanoacrylate) nanoparticles, *Eur. J. Pharm. Biopharm.* 57 (2004) 369–375.
- [22] K. Furumoto, K. Ogawara, S. Nagayama, Y. Takakura, M. Hashida, K. Higaki, T. Kimura, Important role of serum proteins associated on the surface of particles in their hepatic disposition, *J. Control. Release* 83 (2002) 89–96.
- [23] A. Beletsi, Z. Panagi, K. Avgoustakis, Biodistribution properties of nanoparticles based on mixtures of PLGA with PLGA–PEG diblock copolymers, *Int. J. Pharm.* 298 (2005) 233–241.
- [24] B. Pegaz, E. Debeve, J.P. Ballini, Y.N. Konan-Kouakou, H. van den Bergh, Effect of nanoparticle size on the extravasation and the photothrombic activity of meso(*p*-tetracarboxyphenyl)porphyrin, *J. Photochem. Photobiol. B* 85 (2006) 216–222.
- [25] U. Gaur, S.K. Sahoo, T.K. De, P.C. Ghosh, A. Maitra, P.K. Ghosh, Biodistribution of fluoresceinated dextran using novel nanoparticles evading reticuloendothelial system, *Int. J. Pharm.* 202 (2000) 1–10.
- [26] S. Mitra, U. Gaur, P.C. Ghosh, A.N. Maitra, Tumour targeted delivery of encapsulated dextran–doxorubicin conjugate using chitosan nanoparticles as carrier, *J. Control. Release* 74 (2001) 317–323.
- [27] J. Davda, V. Labhasetwar, Characterization of nanoparticle uptake by endothelial cells, *Int. J. Pharm.* 233 (2002) 51–59.
- [28] K. Michaelis, M.M. Hoffmann, S. Dreis, E. Herbert, R.N. Alyautdin, M. Michaelis, J. Kreuter, K. Langer, Covalent linkage of apolipoprotein E to albumin-nanoparticles strongly enhances drug transport into the brain, *J. Pharmacol. Exp. Ther.* (2006).
- [29] X. Sun, R. Rossin, J.L. Turner, M.L. Becker, M.J. Joralemon, M.J. Welch, K.L. Wooley, An assessment of the effects of shell cross-linked nanoparticle size, core composition, and surface PEGylation on in vivo biodistribution, *Biomacromolecules* 6 (2005) 2541–2554.
- [30] K. Avgoustakis, A. Beletsi, Z. Panagi, P. Klepetsanis, E. Livaniou, G. Evangelatos, D.S. Ithakissios, Effect of copolymer composition on the physicochemical characteristics, in vitro stability, and biodistribution of PLGA–mPEG nanoparticles, *Int. J. Pharm.* 259 (2003) 115–127.
- [31] L. Illum, S.S. Davis, R.H. Muller, E. Mak, P. West, The organ distribution and circulation time of intravenously injected colloidal carriers sterically stabilized with a block copolymer – poloxamine 908, *Life Sci.* 40 (1987) 367–374.
- [32] S. Stolnik, B. Daudali, A. Arien, J. Whetstone, C.R. Heald, M.C. Garnett, S.S. Davis, L. Illum, The effect of surface coverage and conformation of poly(ethylene oxide) (PEO) chains of poloxamer 407 on the biological fate of model colloidal drug carriers, *Biochim. Biophys. Acta* 1514 (2001) 261–279.
- [33] M.A. Jepson, N.L. Simmons, D.T. O'Hagan, B.H. Hirst, Comparison of poly(DL-lactide-co-glycolide) and polystyrene microsphere targeting to intestinal M cells, *J. Drug Target.* 1 (1993) 245–249.
- [34] P. Caliceti, F.M. Veronese, Pharmacokinetic and biodistribution properties of poly(ethylene glycol)–protein conjugates, *Adv. Drug Deliv. Rev.* 55 (2003) 1261–1277.
- [35] Y. Takakura, R.I. Mahato, M. Hashida, Extravasation of macromolecules, *Adv. Drug Deliv. Rev.* 34 (1998) 93–108.
- [36] H. Wadenvik, J. Kutti, The spleen and pooling of blood cells, *Eur. J. Haematol.* 41 (1988) 1–5.
- [37] L.W. Seymour, Passive tumor targeting of soluble macromolecules and drug conjugates, *Crit. Rev. Ther. Drug Carrier Syst.* 9 (1992) 135–187.
- [38] L. Cucullo, M.S. McAllister, K. Kight, L. Krizanac-Bengez, M. Marroni, M.R. Mayberg, K.A. Stanness, D. Janigro, A new dynamic in vitro model for the multidimensional study of astrocyte–endothelial cell interactions at the blood–brain barrier, *Brain Res.* 951 (2002) 243–254.
- [39] H.S. Kas, Drug delivery to brain by microparticulate systems, *Adv. Exp. Med. Biol.* 553 (2004) 221–230.
- [40] R.K. Jain, Barriers to drug delivery in solid tumors, *Sci. Am.* 271 (1994) 58–65.
- [41] T. Siegal, A. Horowitz, A. Gabizon, Doxorubicin encapsulated in sterically stabilized liposomes for the treatment of a brain tumor model: biodistribution and therapeutic efficacy, *J. Neurosurg.* 83 (1995) 1029–1037.
- [42] M. Huang, C.W. Fong, E. Khor, L.Y. Lim, Transfection efficiency of chitosan vectors: effect of polymer molecular weight and degree of deacetylation, *J. Control. Release* 106 (2005) 391–406.
- [43] I. Behrens, A.I. Pena, M.J. Alonso, T. Kissel, Comparative uptake studies of bioadhesive and non-bioadhesive nanoparticles in human intestinal cell lines and rats: the effect of mucus on particle adsorption and transport, *Pharm. Res.* 19 (2002) 1185–1193.
- [44] T. Kiang, C. Bright, C.Y. Cheung, P.S. Stayton, A.S. Hoffman, K.W. Leong, Formulation of chitosan–DNA nanoparticles with poly(propyl acrylic acid) enhances gene expression, *J. Biomater. Sci. Polym. Ed.* 15 (2004) 1405–1421.
- [45] Y. Li, M. Ogris, E. Wagner, J. Pelisek, M. Ruffer, Nanoparticles bearing polyethyleneglycol-coupled transferrin as gene carriers:

- preparation and in vitro evaluation, *Int. J. Pharm.* 259 (2003) 93–101.
- [46] J.S. Chawla, M.M. Amiji, Biodegradable poly(epsilon-caprolactone) nanoparticles for tumor-targeted delivery of tamoxifen, *Int. J. Pharm.* 249 (2002) 127–138.
 - [47] T. Ameller, V. Marsaud, P. Legrand, R. Gref, G. Barratt, J.M. Renoir, Polyester-poly(ethylene glycol) nanoparticles loaded with the pure antiestrogen RU 58668: physicochemical and opsonization properties, *Pharm. Res.* 20 (2003) 1063–1070.
 - [48] Y.H. Lin, C.K. Chung, C.T. Chen, H.F. Liang, S.C. Chen, H.W. Sung, Preparation of nanoparticles composed of chitosan/poly-gamma-glutamic acid and evaluation of their permeability through Caco-2 cells, *Biomacromolecules* 6 (2005) 1104–1112.
 - [49] T.K. De, D.J. Rodman, B.A. Holm, P.N. Prasad, E.J. Bergey, Brimonidine formulation in polyacrylic acid nanoparticles for ophthalmic delivery, *J. Microencapsul.* 20 (2003) 361–374.
 - [50] S. Prior, B. Gander, N. Blarer, H.P. Merkle, M.L. Subira, J.M. Irache, C. Gamazo, In vitro phagocytosis and monocyte-macrophage activation with poly(lactide) and poly(lactide-co-glycolide) microspheres, *Eur. J. Pharm. Sci.* 15 (2002) 197–207.
 - [51] S. Salmaso, N. Elvassore, A. Bertucco, A. Lante, P. Caliceti, Nisin-loaded poly-L-lactide nano-particles produced by CO₂ anti-solvent precipitation for sustained antimicrobial activity, *Int. J. Pharm.* 287 (2004) 163–173.
 - [52] C.A. Nguyen, E. Allemann, G. Schwach, E. Doelker, R. Gurny, Cell interaction studies of PLA–MePEG nanoparticles, *Int. J. Pharm.* 254 (2003) 69–72.
 - [53] S. Munier, I. Messai, T. Delair, B. Verrier, Y. Ataman-Onal, Cationic PLA nanoparticles for DNA delivery: comparison of three surface polycations for DNA binding, protection and transfection properties, *Colloids Surf. B Biointerfaces* 43 (2005) 163–173.
 - [54] V.C. Mosqueira, P. Legrand, A. Gulik, O. Bourdon, R. Gref, D. Labarre, G. Barratt, Relationship between complement activation, cellular uptake and surface physicochemical aspects of novel PEG-modified nanocapsules, *Biomaterials* 22 (2001) 2967–2979.
 - [55] I.S. Kim, S.K. Lee, Y.M. Park, Y.B. Lee, S.C. Shin, K.C. Lee, I.J. Oh, Physicochemical characterization of poly(L-lactic acid) and poly(D,L-lactide-co-glycolide) nanoparticles with polyethylenimine as gene delivery carrier, *Int. J. Pharm.* 298 (2005) 255–262.
 - [56] Y. Dong, S.S. Feng, Poly(DL-lactide-co-glycolide)/montmorillonite nanoparticles for oral delivery of anticancer drugs, *Biomaterials* 26 (2005) 6068–6076.
 - [57] A. Weissenböck, M. Wirth, F. Gabor, WGA-grafted PLGA-nanospheres: preparation and association with Caco-2 single cells, *J. Control. Release* 99 (2004) 383–392.
 - [58] P. Ahlin, J. Kristl, A. Kristl, F. Vrecer, Investigation of polymeric nanoparticles as carriers of enalaprilat for oral administration, *Int. J. Pharm.* 239 (2002) 113–120.
 - [59] H.S. Yoo, P.T. Gwan, Biodegradable nanoparticles containing protein–fatty acid complexes for oral delivery of salmon calcitonin, *J. Pharm. Sci.* 93 (2004) 488–495.
 - [60] S. Prabha, W.Z. Zhou, J. Panyam, V. Labhasetwar, Size-dependency of nanoparticle-mediated gene transfection: studies with fractionated nanoparticles, *Int. J. Pharm.* 244 (2002) 105–115.
 - [61] M. Torres-Lugo, M. Garcia, R. Record, N.A. Peppas, Physicochemical behavior and cytotoxic effects of *p*(methacrylic acid-*g*-ethylene glycol) nanospheres for oral delivery of proteins, *J. Control. Release* 80 (2002) 197–205.
 - [62] S. Sakuma, R. Sudo, N. Suzuki, H. Kikuchi, M. Akashi, Y. Ishida, M. Hayashi, Behavior of mucoadhesive nanoparticles having hydrophilic polymeric chains in the intestine, *J. Control. Release* 81 (2002) 281–290.
 - [63] N. Scholer, C. Olbrich, K. Tabatt, R.H. Muller, H. Hahn, O. Liesenfeld, Surfactant, but not the size of solid lipid nanoparticles (SLN) influences viability and cytokine production of macrophages, *Int. J. Pharm.* 221 (2001) 57–67.
 - [64] M.R. Lorenz, V. Holzapfel, A. Musyanovych, K. Nothelfer, P. Walther, H. Frank, K. Landfester, H. Schrezenmeier, V. Mailander, Uptake of functionalized, fluorescent-labeled polymeric particles in different cell lines and stem cells, *Biomaterials* 27 (2006) 2820–2828.
 - [65] C. Fang, B. Shi, Y.Y. Pei, M.H. Hong, J. Wu, H.Z. Chen, In vivo tumor targeting of tumor necrosis factor-alpha-loaded stealth nanoparticles: effect of MePEG molecular weight and particle size, *Eur. J. Pharm. Sci.* 27 (2006) 27–36.
 - [66] Y. Yi, J.H. Kim, H.W. Kang, H.S. Oh, S.W. Kim, M.H. Seo, A polymeric nanoparticle consisting of mPEG–PLA–Toco and PLMA–COONa as a drug carrier: improvements in cellular uptake and biodistribution, *Pharm. Res.* 22 (2005) 200–208.
 - [67] S.E. Gelperina, A.S. Khalansky, I.N. Skidan, Z.S. Smirnova, A.I. Bobruskin, S.E. Severin, B. Turowski, F.E. Zanella, J. Kreuter, Toxicological studies of doxorubicin bound to polysorbate 80-coated poly(butyl cyanoacrylate) nanoparticles in healthy rats and rats with intracranial glioblastoma, *Toxicol. Lett.* 126 (2002) 131–141.
 - [68] Z. Xu, W. Gu, J. Huang, H. Sui, Z. Zhou, Y. Yang, Z. Yan, Y. Li, In vitro and in vivo evaluation of actively targetable nanoparticles for paclitaxel delivery, *Int. J. Pharm.* 288 (2005) 361–368.
 - [69] S.T. Reddy, A. Rehor, H.G. Schmoekel, J.A. Hubbell, M.A. Swartz, In vivo targeting of dendritic cells in lymph nodes with poly(propylene sulfide) nanoparticles, *J. Control. Release* 112 (2006) 26–34.
 - [70] W. Tiyyaboonchai, J. Woiszwillo, R.C. Sims, C.R. Middaugh, Insulin containing polyethylenimine–dextran sulfate nanoparticles, *Int. J. Pharm.* 255 (2003) 139–151.
 - [71] F. De Jaeghere, E. Allemann, R. Cerny, B. Galli, A.F. Steulet, I. Muller, H. Schutz, E. Doelker, R. Gurny, pH-Dependent dissolving nano- and microparticles for improved peroral delivery of a highly lipophilic compound in dogs, *AAPS PharmSci.* 3 (2001).
 - [72] H. Yamamoto, Y. Kuno, S. Sugimoto, H. Takeuchi, Y. Kawashima, Surface-modified PLGA nanosphere with chitosan improved pulmonary delivery of calcitonin by mucoadhesion and opening of the intercellular tight junctions, *J. Control. Release* 102 (2005) 373–381.
 - [73] H.M. Redhead, S.S. Davis, L. Illum, Drug delivery in poly(lactide-co-glycolide) nanoparticles surface modified with poloxamer 407 and poloxamine 908: in vitro characterisation and in vivo evaluation, *J. Control. Release* 70 (2001) 353–363.
 - [74] W.U. Kim, W.K. Lee, J.W. Ryoo, S.H. Kim, J. Kim, J. Youn, S.Y. Min, E.Y. Bae, S.Y. Hwang, S.H. Park, C.S. Cho, J.S. Park, H.Y. Kim, Suppression of collagen-induced arthritis by single administration of poly(lactic-co-glycolic acid) nanoparticles entrapping type II collagen: a novel treatment strategy for induction of oral tolerance, *Arthritis Rheum.* 46 (2002) 1109–1120.
 - [75] L. Costantino, F. Gandolfi, G. Tosi, F. Rivasi, M.A. Vandelli, F. Forni, Peptide-derivatized biodegradable nanoparticles able to cross the blood–brain barrier, *J. Control. Release* 108 (2005) 84–96.
 - [76] M.A. Radwan, H.Y. Aboul-Enein, In vitro release and stereoselective disposition of flurbiprofen loaded to poly(D,L-lactide-co-glycolide) nanoparticles in rats, *Chirality* 16 (2004) 119–125.
 - [77] Z. Panagi, A. Beletsi, G. Evangelatos, E. Livaniou, D.S. Ithakissios, K. Avgoustakis, Effect of dose on the biodistribution and pharmacokinetics of PLGA and PLGA–mPEG nanoparticles, *Int. J. Pharm.* 221 (2001) 143–152.
 - [78] J. Williams, R. Lansdown, R. Sweitzer, M. Romanowski, R. LaBell, R. Ramaswami, E. Unger, Nanoparticle drug delivery system for intravenous delivery of topoisomerase inhibitors, *J. Control. Release* 91 (2003) 167–172.
 - [79] K. Ogawara, K. Furumoto, S. Nagayama, K. Minato, K. Higaki, T. Kai, T. Kimura, Pre-coating with serum albumin reduces receptor-mediated hepatic disposition of polystyrene nanosphere: implications for rational design of nanoparticles, *J. Control. Release* 100 (2004) 451–455.
 - [80] R.L. Conhaim, A. Eaton, N.C. Staub, T.D. Heath, Equivalent pore estimate for the alveolar-airway barrier in isolated dog lung, *J. Appl. Physiol.* 64 (1988) 1134–1142.
 - [81] K.E. Arfors, G. Rutili, E. Svensjo, Microvascular transport of macromolecules in normal and inflammatory conditions, *Acta Physiol. Scand. Suppl.* 463 (1979) 93–103.